Colloidal binary mixtures at fluid-fluid interfaces under steady shear: structural, dynamical and mechanical response - Electronic Supplementary Information

Ivo Buttinoni, Zachary A. Zell, Todd M. Squires, and Lucio Isa

1 PARTICLE TRACKING AND COMPUTATION OF THE VELOCITIES

The velocities of the particles are usually extracted from experimental snapshots by means of particle tracking algorithms (PT). We analyze the recorded image sequences using custom Matlab codes, extract the positions of the particles at each frame and reconstruct the trajectories connecting nearest coordinates in consecutive frames. This strategy leads to the desired results provided that the displacements of the particles between two consecutive frames do not exceed the typical inter-particle distance. A simple estimate leads to the following condition for a successful tracking.

$$\omega(r)r < \frac{\pi d\chi}{8\phi}, \tag{1}$$

where $\omega(r)$ is the local angular velocity at distance r from the disk center, d is the particle diameter, ϕ is the area fraction and χ is the acquisition frame rate. The velocity profiles in the regions where Eq. (1) is not satisfied are computed by means of the image correlation method (IC) illustrated in Figure 1. In short, we consider two consecutive frames (Fig. 1(a) and (b)), isolate the coronas that correspond to the particles layers (e.g., the region marked in red), rotate them by different angles and find the angle $\Delta\theta$ that maximizes the correlation ρ between the highlighted areas of the images (see Fig. 1(c)). The angle $\Delta\theta$ corresponds to the average angular velocity at distance r. Of course, the method described above has physical meaning as long as the particles travel with the mean flow, i.e., in what we defined as Flowing regime (FR). This is the case of our experiments since we employ IC only at close distances from the probe and for rotational

frequencies of the probe larger than 2 Hz. Finally, we remark that, in the regions where both particle tracking and image correlation can be applied, the two methods lead to similar results as shown in the main paper. We also report no correspondence between the method employed and the FR-HR transition.

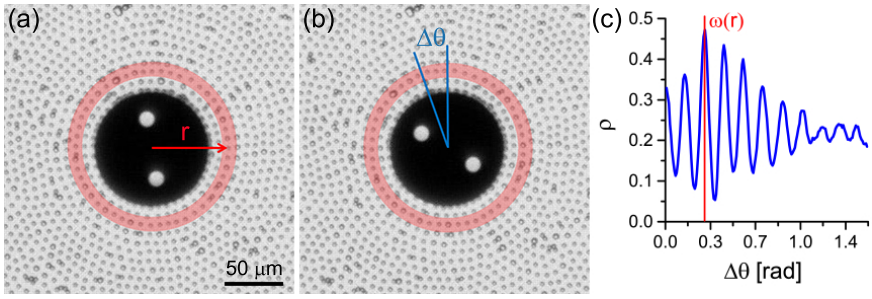

Figure 1: (a-b) Experimental snapshots corresponding to two consecutive frames when the magnetic probe rotates at 8 Hz. According to the IC method, the angular velocity at distance r is given by the rotation angle $\Delta\theta$ corresponding to the maximum correlation coefficient ρ between the red coronas (c).

2 VELOCITY PROFILES: DATA AT DIFFERENT AREA FRACTIONS

Measured velocity profiles and normalized standard deviations for bidisperse monolayers at various surface concentrations, cited in the main paper, are shown in Figure 2.

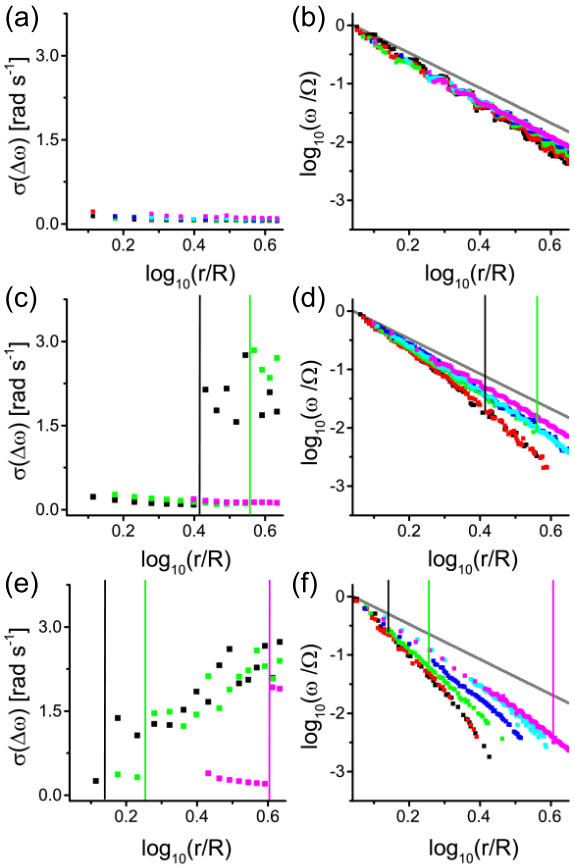

Figure 2: Normalized standard deviation of the angular velocity distributions (a,c,e) and log-log plots of the normalized angular velocities (b,d,f) for bidisperse monolayers with area fraction ϕ sheared at frequency Ω. Only three frequencies Ω are shown in (a), (c) and (e) for clarity. (a,b) $\phi = 0.04$. $\Omega/2\pi$ =0.3 (black), 0.5 (red), 1 (green), 2 (blue), 4 (cyan), 7 (magenta) Hz. (c,d) $\phi = 0.09$. $\Omega/2\pi$ =0.3 (black), 0.5 (red), 1 (green), 1.5 (blue), 2 (cyan), 5 (magenta) Hz. (e,f) $\phi = 0.19$. $\Omega/2\pi$ =0.3 (black), 0.5 (red), 1 (green), 2 (blue), 5 (cyan), 7 (magenta) Hz. The slope of the power-law FR region changes with Ω and ϕ and becomes close to 3 (grey analytical curve in (b), (d) and (f)) at large frequencies and small area fractions.

3 MONODISPERSE MONOLAYERS

Fig. 3(a) shows the velocity profiles for a monolayer made of large particles only (diameter $d_B = 4$ μm). The corresponding surface viscosity plot is illustrated in Fig. 3(b). Comparison with a bidisperse monolayer at similar area fraction reveals no significant difference in the mechanical response.

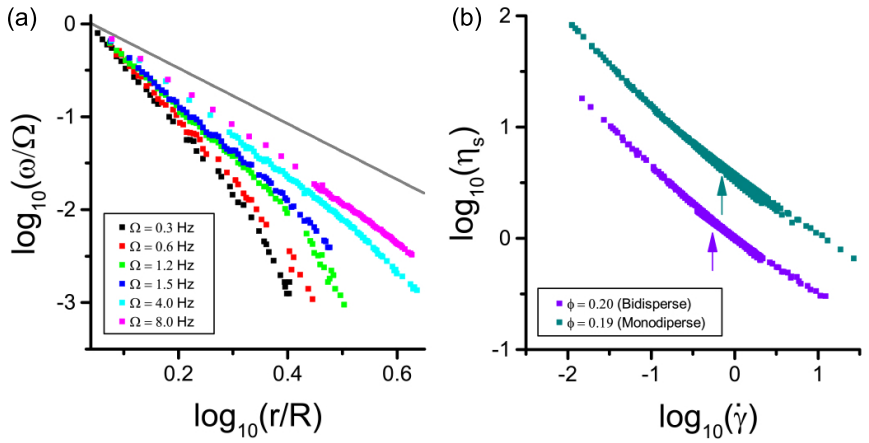

Figure 3: (a) Log-log plots of the normalized angular velocities for a monodisperse monolayer with $\phi = 0.19$ sheared at different frequencies Ω. (b) Log-log plots of the surface viscosity of monodisperse and bidisperse monolayers with similar ϕ.

4 MICROPROBES WITH DIFFERENT GEOMETRIES

The geometry of the magnetic probe affects the flow field only at very close distances from the probe edge (see Fig 4).

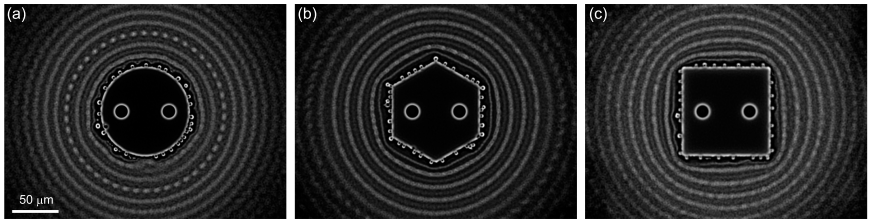

Figure 4: Long-exposure images of binary monolayers sheared at 3 Hz using circular (a), hexagonal (b) and square (c) probes. After a few layers away from the disk, the circular symmetry of the flow-induced structures is recovered.